World Academy of Science, Engineering and Technology
International Journal of Civil and Environmental Engineering
Vol:8, No:9, 2014

Effect of Tube Thickness on the Face Bending for Blind-Bolted Connection to Concrete Filled Tubular Structures

Mohammed Mahmood, Walid Tizani, Carlo Sansour

***Abstract*—**In this paper, experimental testing and numerical analysis were used to investigate the effect of tube thickness on the face bending for concrete filled hollow sections connected to other structural members using Extended Hollobolts. Six samples were tested experimentally by applying pull-out load on the bolts. These samples were designed to fail by column face bending. The main variable in all tests is the column face thickness. Finite element analyses were also performed using ABAQUS 6.11 to extend the experimental results and to quantify the effect of column face thickness. Results show that, the column face thickness has a clear impact on the connection strength and stiffness. However, the amount of improvement in the connection stiffness by changing the column face thickness from 5mm to 6.3mm seems to be higher than that when increasing it from 6.3mm to 8mm. The displacement at which the bolts start pulling-out from their holes increased with the use of thinner column face due to the high flexibility of the section. At the ultimate strength, the yielding of the column face propagated to the column corner and there was no yielding in its walls. After the ultimate resistance is reached, the propagation of the yielding was mainly in the column face with a miner yielding in the walls.

***Keywords*—**Anchored bolted connection, Extended Hollobolt, Column faces bending and concrete filled hollow sections.

I. Introduction

THE blind bolting or single side connection system was introduced to perform a practical connection to Structural Hollow Sections (SHS). During the last period, different types of blind bolts have been introduced. The column face of SHS was the main component responsible for resisting the connection load. Within wide range of SHS, the column face bending limits the capacity of the connection [1]-[4] (Fig. 1).

Filling the SHS with concrete was suggested as a solution to improve the column face behaviour. It can increase the strength and stiffness of the connection by reducing the column face deformations in both tension and compression sides as well as providing fixed support for the column face at the column sidewalls by eliminating the deformations at column sidewalls [5].Some researchers described the effect of concrete infill as increasing the column plate thickness [6]. However, even with concrete infill the column face remains controlling the connection strength in the majority of SHS.

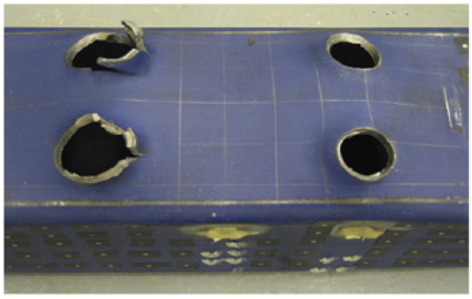

Fig. 1 Column face failure [4]

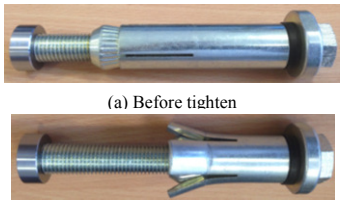

(a) Before tighten

(b) After tighten

Fig. 2 Extended Hollobolt

Tizani and Ridley-Ellis [7] tried to obtain more benefits from concrete by developing a promising blind bolting system called Extended Hollobolt (EHB) (Fig. 2). This bolt was developed to improve the connection stiffness and strength by involving the concrete not only in supporting the column walls and face in compression side but in the pull-out resistance of the bolt by anchoring part of the EHB inside the concrete. EHB has quite comparable behaviour to the standard bolt in terms of failure mode and capacity and it was proven to be used adequately as moment resisting connection [8]. The EHB connection behaviour was controlled by the bolt strength with use of rigid column face [9]. However, with the flexible column face the strength could be controlled by the column face failure. The aim of this research is to study the effect of column face thickness on its bending behaviour as a connection component through experimental testing and numerical analysis.

II. Experimental Programme

The experimental programme is composed of performing pull-out tests for single row of EHBs from concrete filled

Mohammed Mahmood, PhD student, Faculty of Engineering, The University of Nottingham, UK (e-mail: evxmema@nottingham.ac.uk), Lecturer, Department of Civil Engineering, University of Diyala, Iraq.

Walid Tizani, Associate Professor in Structural Engineering Design and Informatics, Faculty of Engineering, The University of Nottingham, UK (e-mail: walid.tizani@nottingham.ac.uk).

Carlo Sansour, Professor of Civil Engineering, The University of Nottingham, UK (e-mail: carlo.sansour@nottingham.ac.uk).

SHS. The basic components of the tested samples are SHS, concrete infill and EHB. This study focuses on investigating the effect of the column face thickness on its bending behaviour. Therefore, the main variable in all tests is the column face thickness. Dummy M16 EHBs were used instead of the real EHBs to eliminate any high deformation of the EHBs that might exist during the test and also to limit the failure at the column face. EHBs were manufactured form high quality, high tensile alloy steel (EN24). The geometry of the dummy EHBs is exactly similar to the totally opened sleeve EHB [10]. The sample length is 760mm; this length is enough to eliminate any interaction between the column face bending and the reaction forces at the sample ends. The test setup is presented in Fig. 3.

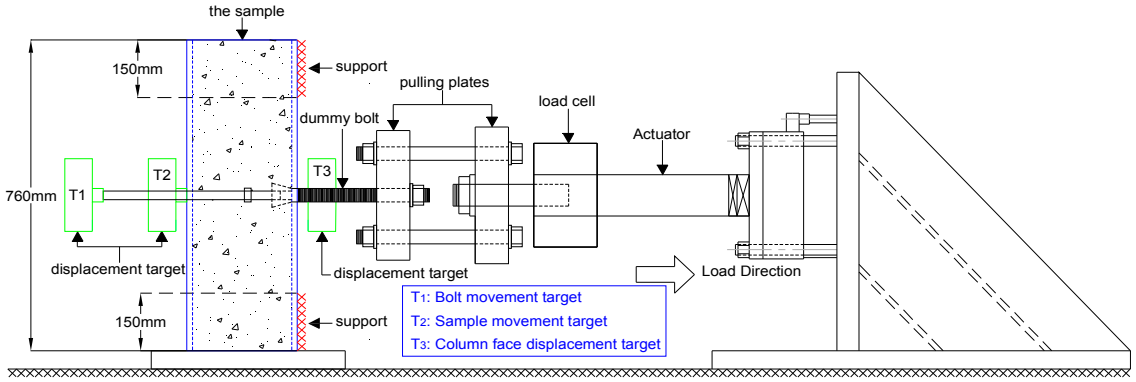

Fig. 3 Test setup

Pull-out load is applied to the dummy EHBs with a loading rate of 0.015 mm/sec. During the test, the column face displacement was monitored to evaluate the strength and stiffness of the column face and the bolt movement was recorded to identify the bolt pull-out point. Recording the bolt movement requires attaching a threaded M16 rod to the end of the EHB. To eliminate any interaction between this rod and the concrete, M20 steel tube was used to cover the rode until the concrete hardening. The sample setup is presented in Fig. 4.

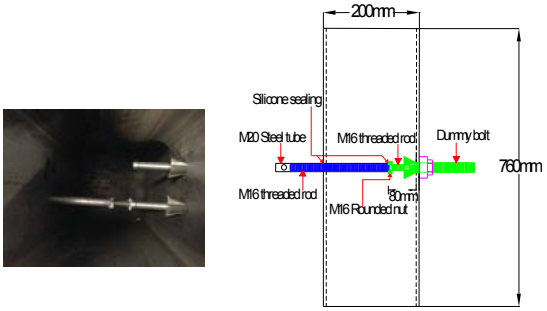

Fig. 4 Samples details

A video gauge system was used to record the column face displacement (Δ_f), bolt movement (Δ_b) and the sample movement at the bolts level (Δ_s). This system can measure a wider range of displacement compared with the linear potential meter and it was proven to provide accurate results by comparing its readings with the linear potential meter readings [9]. The net column face displacement (Δ_{fn}) and the net bolt movement (Δ_{bn}) are calculated using the following equations.

$$\Delta_{fn} = \Delta_f - \Delta_s \quad (1)$$

$$\Delta_{bn} = \Delta_b - \Delta_s \quad (2)$$

The effect of the column face thickness (t) will be discussed here as the slenderness ratio of the column face (ratio of the column face width to its thickness, $\mu=\frac{b}{t}$). The column face with μ equal to 20 was confirmed to behave as a rigid plate with no signs of yielding at the face of concrete filled SHS until the failure of the EHBs [8], [9]. Therefore, in this study the minimum value of μ is 25 to have flexible column face. The maximum value of μ is 40, which was specified based on the Euro code [11] requirements for preventing local buckling failure of steel-concrete composite sections. 200×200×8 ($\mu=25$), 200×200×6.3 ($\mu=31.75$) and 200×200×5 ($\mu=40$) SHS were tested to cover the range of the slenderness ratio. The actual dimensions and the holes size are listed in Table I.

TABLE I
ACTUAL SECTION DIMENSIONS AND HOLES SIZE

	μ40-1	μ40-2	μ31.75-1	μ31.75-2	μ25-1	μ25-2
Section width (b) mm	200	200	201	201	200	200
Plate thickness (t) mm	4.94	4.94	6.35	6.35	7.99	7.98
Corner thickness (t_c) mm	5.6	5.59	7.36	7.36	8.72	8.71
Hole diameter (D) mm	26.76	26.75	26.94	26.95	26.75	26.74

The tests were performed for two identical samples for each slenderness ratio to eliminate any unrealistic results. All the tests were performed with a bolt gauge distance equal to 80mm and bolt anchorage length of 80mm. The concrete infill for all the tests was prepared using same concrete mix. The concrete strength in the day of test was 38, 36 and 41.3 N/mm^2 for slenderness ratio of 40, 31.75 and 25 respectively.

The mechanical properties of the SHS were obtained from the coupon tensile test. The geometry and the test procedure were according to EN 10002-1:2001[12]. The yield strength

(f_y), the ultimate strength (f_u), Yong's modulus of elasticity (E_s) for each SHS are listed in Table II and also the complete stress-strain data were recorded.

TABLE II
MATERIAL PROPERTIES FOR THE TESTED SAMPLES

Sample ID	Concrete strength f_{cu} (N/mm^2)	Yield strength f_y (N/mm^2)	Ultimate strength f_u (N/mm^2)	Young's modulus E_s (N/mm^2)
µ40-1	38	433	547	180000
µ40-2	38	433	547	180000
µ31.75-1	36	413	548	191000
µ31.75-2	36	413	548	191000
µ25-1	41.3	406	537	207000
µ25-2	41.3	406	537	207000

III. EXPERIMENTAL RESULTS

The column face load carrying capacity versus displacement is presented in Fig. 5 for all the tested samples. The behaviour is approximately linear until the maximum capacity and after which there is a drop in the resistance. This drop might be attributed to the loss of bond between the concrete and EHB due to the high deformation. Results indicate that, there are significant improvements in ultimate load carrying capacity and the stiffness of the column face with the use of thicker column face. However, the stiffness of the column face is more sensitive to the column face thickness than the column face strength.

Fig. 6 shows comparison of column face displacement and bolt movement curves for all the samples. With the thin section the bolt and column face were moving together at the same load and displacement for long part of the curve (about 8mm) before the bolt starts pulling-out. This part was reduced with use of thicker sections to become 4mm and 3mm for 6.3mm and 8mm thickness respectively. There was also decrease in the pull-out displacement with the increase of the column face thickness. This could be due to flexibility of the column face with high slenderness ratio, whereas with low slenderness ratio the column face behaviour moves towards rigid plates so that the bolt starts pulling-out in lower displacement. Table III summarizes the pull-out displacements for all samples.

TABLE III
PULL-OUT DISPLACEMENTS

	µ40-1	µ40-2	µ31.75-1	µ31.75-2	µ25-1	µ25-2
Column face displacement (mm)	12.036	12.083	11.177	11.192	11.061	11.030

However, part of these variations in the behaviour might be attributed to the differences in the mechanical properties for concrete and steel for the tested samples. Therefore, Finite Element (FE) analysis was performed in this study to quantify the effect of the column face only on the connection behaviour.

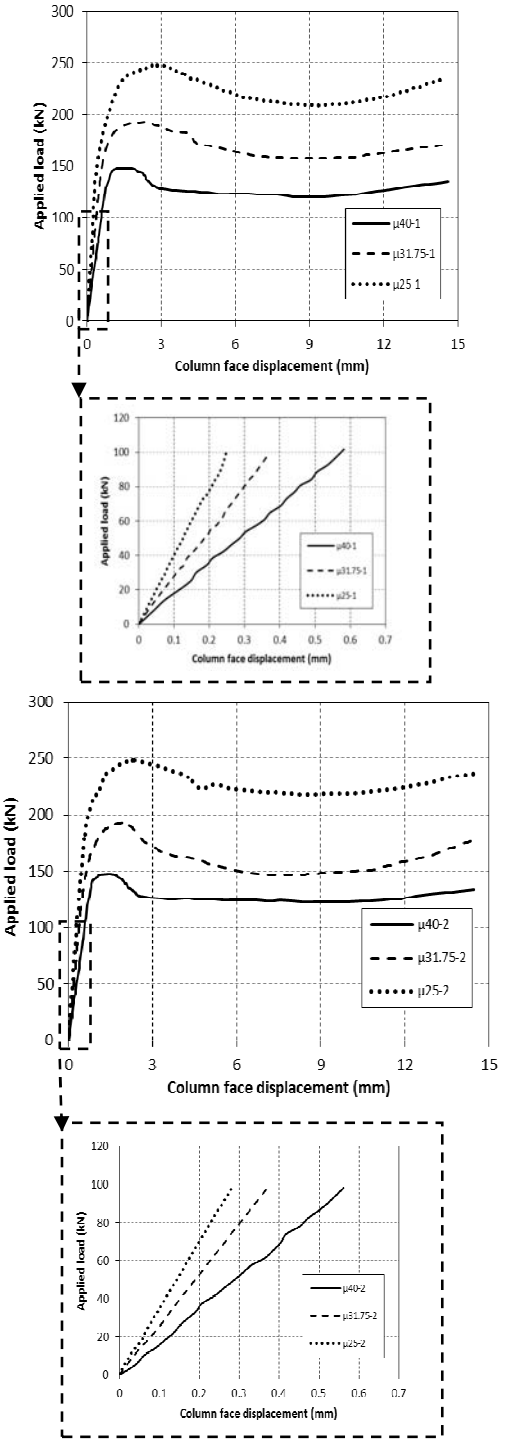

Fig. 5 Applied load versus the column face displacement curves for µ40, µ31.75 and µ25

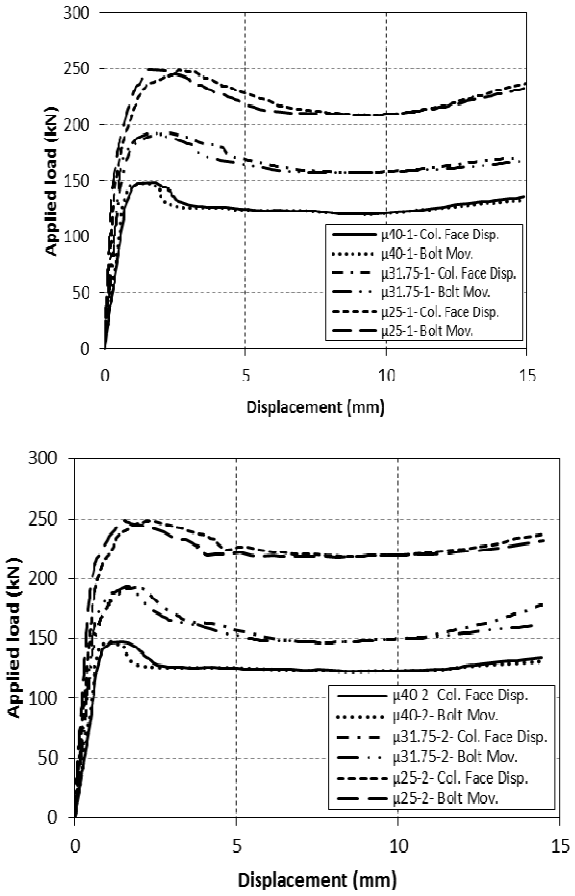

Fig. 6 Column face displacement and bolt movement curves for μ40, μ31.75 and μ25

The Digital Image Correlation (DIC) system was used to monitor the strain distribution in the column face during the testing of μ25-1 and μ25-2. It is an optical measuring instrument for true full field, non-contact and three-dimensional analysis of displacements and strains on components and specimens. Due to the limited view to the column face during the test, only the area enclosed by the red lines in Fig. 7 was monitored.

Fig. 7 Area captured by DIC system

The first yielding's sing was recorded at 71% of the ultimate load and it was at the hole edge. At the ultimate load carrying capacity, the SHS corner starts yielding. After the ultimate resistance and until the test end, the propagation of the yield was mainly in the column face. Strain development on the column face is presented in Fig. 8.

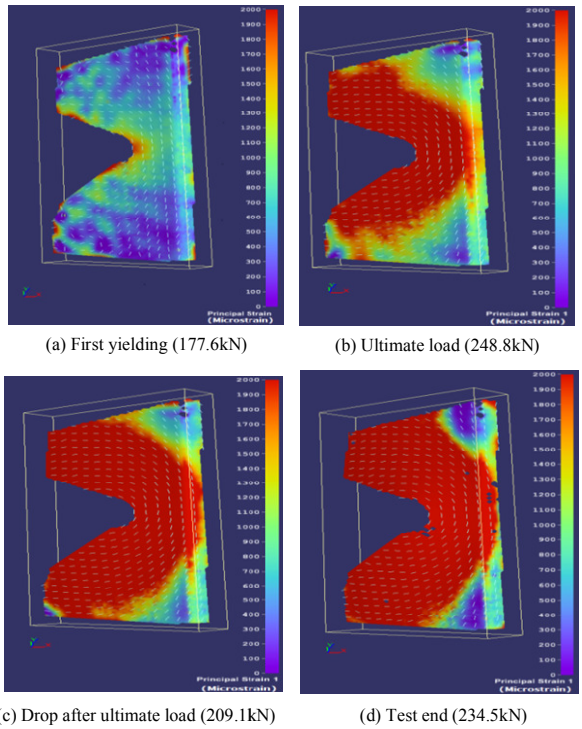

(a) First yielding (177.6kN) (b) Ultimate load (248.8kN)

(c) Drop after ultimate load (209.1kN) (d) Test end (234.5kN)

Fig. 8 Strain development on the column face

IV. Finite Element Model

The general purpose Finite Element (FE) package ABAQUS 6.11 [13] was adopted to simulate the tested samples. The model consists of three components: SHS, concrete and EHBs. All the components were modelled using three dimensional continuum eight nodes element (C3D8). This element is suitable for modelling the complex nonlinear behaviour and involving contact and geometrical nonlinearities [14].

The contact between the different parts of the model was simulated using surface to surface contact algorithm. Both hard and tangential contacts were exciting in the model. The friction coefficient between EHBs and the concrete is 0.25 [15]-[17] and between EHBs and the hole is 0.45 [18].

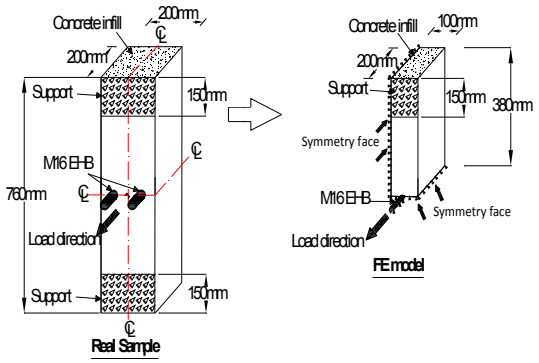

Fig. 9 FE Model geometry

The tested samples are symmetric along their longitudinal and transverse axes. Therefore, only quarter of the model was simulated. The details of the whole sample and the FE model are presented in Fig. 9.

A. Modelling the SHS

The measured geometrical properties listed in Table I were fed to the FE model to achieve acceptable level of accuracy. The elastic behaviour of each SHS was simulated by the Young's modulus of elasticity (Table II) and Poison's ratio of 0.3. The stress strain values obtained from the coupon tests were used to model the plastic behaviour of the SHS. However, the stress and strain that were obtained from these tests are engineering values (they are calculated based on the undeformed cross-section). Therefore, all the test results were transferred to true values using (3) and (4) before using them in the FE model [14].

$$\sigma_{true} = \sigma_{nom}(1 + \varepsilon_{nom}) \quad (3)$$

$$\varepsilon_{true} = \ln(1 + \epsilon_{nom}) \quad (4)$$

where σ_{true} : true stress, σ_{nom} : nominal or engineering stress, ε_{nom} : nominal or engineering strain and ε_{true} : true train

B. Modelling the Concrete

The concrete linear behaviour was simulated using the elastic model by defining its Young's modulus of elasticity (E_c) and Poison's ratio. Equation (5) [19] was used to calculate E_c and the Poison's ratio was considered as 0.2.

$$E_c = 22000\left(\frac{f_c'}{10}\right)^{0.3} \quad (5)$$

where E_c : concrete Young's modulus (N/mm^2) and f_c' : characteristic compressive cylinder strength (N/mm^2)

The plastic behaviour of concrete was modelled using the Concrete Damage Plasticity (CDP) model. The failure mechanism for this model is compatible with concrete behaviour (tensile cracking and compression crushing). The concrete compression stress-strain relation was defined using the multi-linear model proposed by BSI [19]. However, the ultimate concrete compressive strength is considered equal to the characteristic compressive cylinder strength of concrete (f_c') instead of (f_c'+8). This model assumes linear behaviour of the concrete until 40% of f_c'. Then a nonlinear ascending curve starts until reaching the ultimate concrete strength and after the peak point there is a descending part in the curve until a strain equal to ε_{c2}. In this study, the curve at strain range between ε_{c1} and ε_{c2} was regarded as stable plateau to avoid numerical problems in finite element analysis (Fig. 10 (a)). The stress-strain values are calculated using the following equations:

$$f_c = \left(\frac{k\eta - \eta^2}{1+(k-2)\eta}\right) f_c' \quad (6)$$

$$k = \frac{1.05\, E_c \varepsilon_{c1}}{f_c'} \quad (7)$$

$$\varepsilon_{c1} = \frac{0.7(f_c')^{0.31}}{1000} < 0.0028 \quad (8)$$

$$\varepsilon_{c2} = 0.0035 \quad \text{for } f_c' \le 50N/mm^2 \quad (9)$$

$$\eta = \frac{\varepsilon_c}{\varepsilon_{c1}} \quad (10)$$

where f_c : concrete compressive stress at any point on the stress-strain curve (N/mm^2), E_c : concrete Young's modulus (N/mm^2), f_c' : characteristic compressive cylinder strength (N/mm^2), ε_{c1}: concrete compressive strain at the maximum stress (f_c'), ε_{c2}: concrete compressive strain at the at the end of stress-strain curve and ε_c : compressive strain in the concrete.

The tensile behaviour of concrete was simulated using bilinear model. The ultimate tensile strength (f_t)was assumed equal to %10 of f_c' (Fig. 10 (b)).

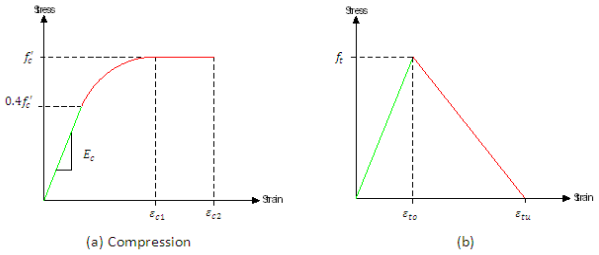

Fig. 10 Concrete Compressive and tension stress- strain curves used in this study

In addition to the stress-strain relations and the damage parameters, CDP requires appropriate plasticity parameters. Table IV presents the values of the plasticity parameters that have been used in the present study.

TABLE IV
PLASTICITY PARAMETERS

dilation angle (φ)	eccentricity (ϵ)	σ_{bo}/σ_{co}	yield shape parameter (k_c)	viscosity parameter (μ_o)
35°	0.1	1.16	1	0

C. Modelling the EHB

The geometry of the EHB in the FE model is exactly similar to the Dummy EHBs used in the experimental tests. This bolt was manufactured from high strength steel so that the maximum load that might be applied during the test is always less than its yield strength. Therefore the EHBs were modelled as an elastic material only.

V. FE Model Validation

In order to verify the accuracy of the numerical model, its results were compared with experimental data and observations. Fig. 11 shows a comparison between the experimental and numerical load versus the column face displacement for all the samples. The general pattern of the FE curves has good correlation with the experimental data. However, after the ultimate load carrying capacity the FE model shows stronger behaviour than the experimental due to the limited simulated damage in the concrete model.

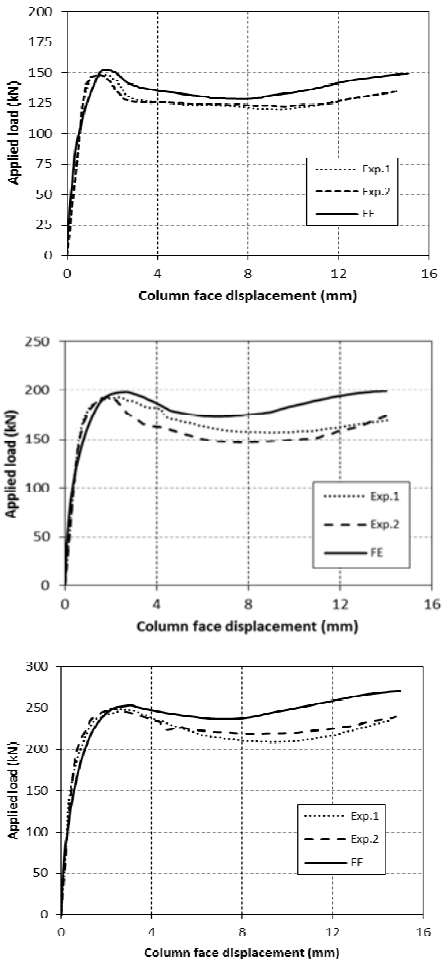

Fig. 11 Load displacement curves Experimental versus FE

Table V summarizes a comparison between the maximum load carrying capacity (the peak load before the drop) of the column face from experimental tests and FE analysis. The FE model seems to be stronger than the real samples. However, the maximum difference was 2.7%.

TABLE V
ULTIMATE LOAD CARRYING CAPACITY OF THE COLUMN FACE EXPERIMENTAL AND FE RESULTS

Sample	Max. load (kN)		% Difference
	Experimental	FE	
µ40-1	147.972	152.015	2.7
µ40-2	147.635	152.015	3
µ31.75-1	192.592	197.834	2.7
µ31.75-2	193.405	197.834	2.3
µ25-1	248.814	252.815	1.6
µ25-1	248.365	252.815	1.8

The strain distribution in the column face was also considered as a validation parameter (Fig. 12). There was good agreement between the FE and the experimental results in terms of values and the yield pattern.

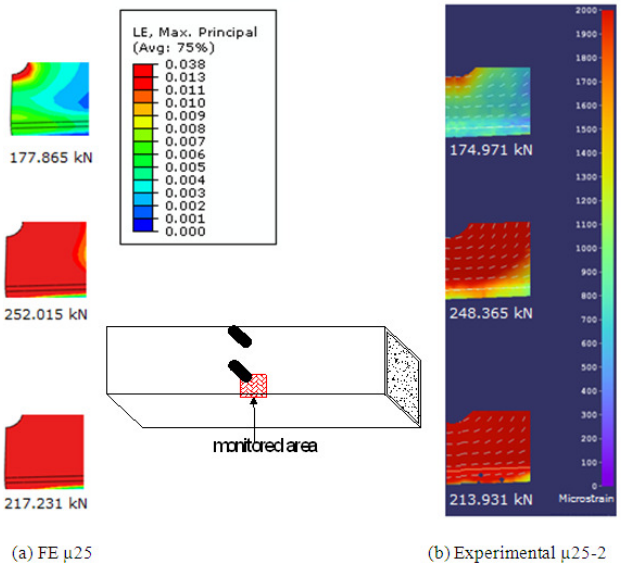

Fig. 12 Strain distribution in the column face (DIC and FE results)

VI. FINITE ELEMENT RESULTS ANALYSIS

The SHS used in the FE analysis is 200X200 with three different thicknesses 5mm, 6.3mm and 8mm. These are the only available sections in the practical range of SHS that could be used in building industry with flexible column face. For all analysis cases, the bolt gauge distance and the bolt anchorage length are 80mm. The SHS mechanical properties are assumed to be similar to µ31.75-1 and the concrete strength is 40N/mm^2.

Fig. 13 shows the effect of column face thickness on its bending behaviour. It is clear that the column face thickness has great impact on both the strength and the stiffness. However, the amount of improvement in the stiffness by changing the column face thickness from 5mm to 6.3mm seems to be higher than that when increasing it from 6.3mm to 8mm. The explanation for this behaviour might be because all the samples have same concrete strength, which has specific capacity and it starts losing its contribution in the load resistance at certain load level. This is confirmed by monitoring the first signs of concrete crushing, which was found concentrated around the anchored nut (Fig. 14). The crushing identified when the strain in concrete reaches its plastic value. The crushing of concrete started at load level of 21% from the maximum load carrying capacity for the sample with column thickness equal to 5mm. This percent is increased to 26 with use of 6.3mm column face thickness, which means there is a good distribution in the resistance between the concrete and the column face. However, the percent dropped again to 21 with column face thickness equal to 8mm. This means there should be a balance between the concrete strength and column face thickness to obtain the optimum behaviour for the two materials and this needs further investigations to find this optimum combination.

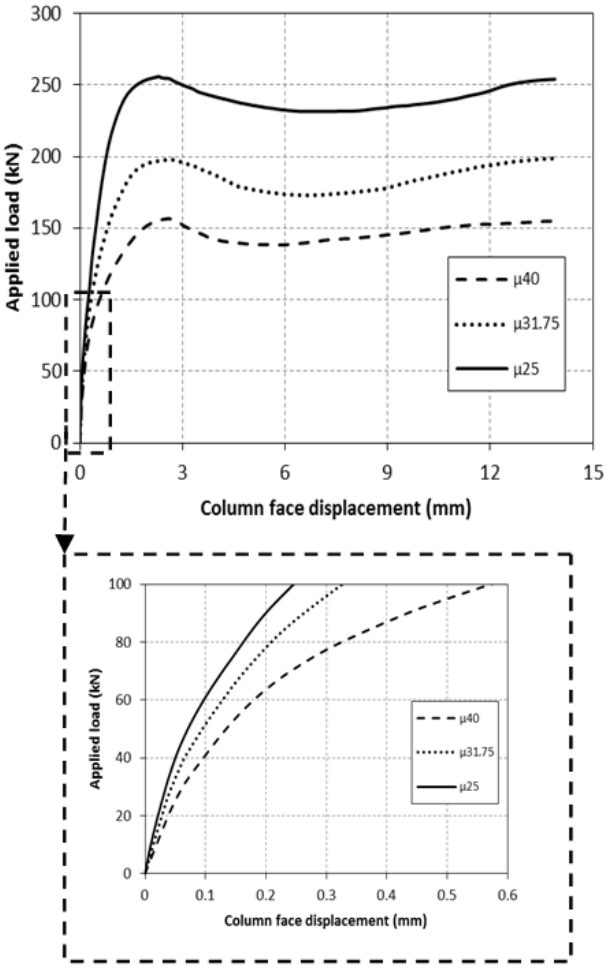

Fig. 13 Column face behaviour for various column face thickness

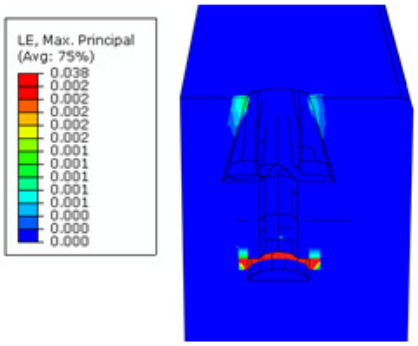

Fig. 14 Concrete crushing

VII. Conclusions

The effect of column face thickness on its bending behaviour in EHB connection was investigated using both experimental and numerical methods. In the absence of the flexibility of the EHB, the behaviour of all the tested samples was approximately linear up to the ultimate strength. Then the column face resistance was dropped due to the loss of bonding between the concrete and dummy EHB. The column face thickness could affect the connection strength and stiffness significantly. However, there should be an optimal combination between the column face thickness and the concrete strength to achieve the best performance for the column face and the concrete and this is the subject for future work.

Acknowledgment

The first author would like to thank the higher committee for education development in Iraq for providing the chance to perform this research.

References

[1] E. Mourad, Behaviour of Blind Bolted Moment Connections for Square HSS Columns. School of Graduated Studies, 1993. PhD Thesis. McMaster University.
[2] T. Barnett, The Behaviour of a Blind Bolt for Moment Resisting Connections in Hollow Steel Sections. Civil Engineering, 2001. Ph. D. Thesis. University of Nottingham.
[3] J.E. France, Bolted Connections between Open Section Beams and Box Columns. Department of Civil and Structural Engineering, 1997. PhD Thesis. University of Sheffield.
[4] J. Lee, H.M. Goldsworthy, and E.F. Gad, Blind Bolted T-Stub Connections to Unfilled Hollow Section Columns in Low Rise Structures. Journal of Constructional Steel Research, 2010. 66(8–9): p. 981-992.
[5] L. Silva, L. Neves, and F. Gomes, Rotational Stiffness of Rectangular Hollow Sections Composite Joints. Journal of Structural Engineering, 2003. 129: p. 487-494.
[6] J.E. France, J. Buick Davison, and P. A. Kirby, Moment-Capacity and Rotational Stiffness of Endplate Connections to Concrete-Filled Tubular Columns with Flowdrilled Connectors. Journal of Constructional Steel Research, 1999. 50(1): p. 35-48.
[7] S. Ellison and W. Tizani, Behaviour of Blind Bolted Connections to Concrete Filled Hollow Sections. The Structural Engineer, 2004. 16: p. 16-17.
[8] W. Tizani, A. Al-Mughairi, J.S. Owen, and T. Pitrakkos, Rotational Stiffness of a Blind-Bolted Connection to Concrete-Filled Tubes Using Modified Hollo-Bolt. Journal of Constructional Steel Research, 2013. 80: p. 317-331.
[9] T. Pitrakkos and W. Tizani, Experimental Behaviour of a Novel Anchored Blind-Bolt in Tension. Engineering Structures, 2013. 49: p. 905-919.
[10] A. Elamin, The Face Bending Behaviour of Blind-Bolted Connections to Concrete-Filled Hollow Sections. Department of Civil Engineering 2013. PhD Thesis. University of Nottingham.
[11] CEN, Eurocode 4: Design of Composite Steel and Concrete Structures: Part 1-1: General Rules and Rules for Buildings, in EN 1994-1-1. 2004.
[12] BSI, Metallic Materials -Tensile Testing, Part 1: Method of Test at Ambient Temperature, in EN 10002-1. 2001, British Standards Institution: London.
[13] Dassault, Abaqus v. 6.11 (Software), Dassault Systèmes Simulia Corp. 2011, Providence, RI: Dassault Systèmes Simulia Corp.
[14] Abaqus, ABAQUS Analysis User's Manual: Volume IV: Elements, in Abaqus, Inc. 2011, Dassault Systèmes.
[15] A. Elremaily and A. Azizinamini, Design Provisions for Connections between Steel Beams and Concrete Filled Tube Columns. Journal of Constructional Steel Research, 2001. 57(9): p. 971-995.
[16] H.T. Hu, C.S. Huang, M.H. Wu, and Y.M. Wu, Nonlinear Analysis of Axially Loaded Concrete-Filled Tube Columns with Confinement Effect. Journal of Structural Engineering, 2003. 129(10): p. 1322-1329.
[17] E. Ellobody, B. Young, and D. Lam, Behaviour of Normal and High Strength Concrete-Filled Compact Steel Tube Circular Stub Columns. Journal of Constructional Steel Research, 2006. 62(7): p. 706-715.
[18] Z. Wang, Hysteretic Response of an Innovative Blind bolted Endplate Connection to Concrete Filled Tubular Columns. Department of Civil Engineering, 2012. PhD Thesis. University of Nottingham.
[19] BSI, Eurocode 2: Design of Concrete Structures: Part 1-1: General Rules and Rules for Buildings, in EN 1992-1-1. 2004, British Standards Institution.